SCIEPublish

Article

Bio-Based Production of Uroporphyrin in *Escherichia coli*

Bahareh Arab, Adam W. Westbrook, Murray Moo-Young, Yilan Liu and C. Perry Chou *

Department of Chemical Engineering, University of Waterloo, Waterloo, ON N2L 3G1, Canada; barab@uwaterloo.ca (B.A.); westbrookaw1@gmail.com (A.W.W.); mooyoung@uwaterloo.ca (M.M.-Y.); yilan.liu@uwaterloo.ca (Y.L.)

* Corresponding author. E-mail: cpchou@uwaterloo.ca (C.P.C.)

Received: 14 December 2023; Accepted: 1 February 2024; Available online: 6 February 2024

Abstract: Uroporphyrin (UP) is a porphyrin compound with medical applications and a key precursor for heme biosynthesis. However, there is no biosynthetic strategy for UP production. In this study, we present a novel bioprocess for enhanced production of UP in engineered *Escherichia coli*. We first implemented the Shemin/C4 pathway heterologously in an *E. coli* strain with an enlarged intracellular pool of succinyl-CoA. Using a plasmid with the *trc* promoter regulating the expression of a synthesized gene operon, the effects of key pathway genes, including *hemA*, *hemB*, *hemC*, and *hemD*, on UP biosynthesis were characterized. By cultivating the resulting engineered *E. coli* strains in a batch bioreactor with 30 g/L glycerol under aerobic conditions, up to 901.9 mg/L UP was produced. Most of the synthesized UP was extracellularly secreted with a high purity more than 80 wt%, facilitating its downstream purification. The study paves the way for large-scale bio-based production of UP using synthetic biology and metabolic engineering strategies.

Keywords: Bio-based production; *Escherichia coli*; Metabolic engineering; Shemin pathway; Tetrapyrrole biosynthetic pathway; Uroporphyrin

1. Introduction

Porphyrins are a group of colorful chemical compounds with an interconnected tetrapyrrole structure [1]. Among them, heme and chlorophyll are the two most well-known members which respectively give red color to blood and green color to plants, algae, and cyanobacteria. Due to versatile and novel applications in various sectors, including therapeutics, molecular electronics, and polymers, porphyrins have gained significant interest [2,3]. Currently, most porphyrins are produced through chemical synthesis [4–6]. Extraction from natural sources such as animal tissues and plants are also reported [7,8]. However, the chemical methods might not be technologically effective and environmentally friendly, and often result in low yields with no selective production of specific porphyrin isomers [9,10]. Extraction from biological sources is also limited by low yield, seasonal variations, and complexities in purification [11]. The complex downstream processing for porphyrin purification further impacts the efficiency and economic feasibility of these methods. Bio-based production, which has been recognized as a more sustainable approach for the production of many value-added chemicals and fuels [12], can offer a potential solution to overcome these limitations. Bio-based systems have potentials for continuous production, thereby reducing time and resource consumption. Their scalability, higher yields, and reduced environmental impact make them a promising alternative to traditional methods.

Heme biosynthesis is highly conserved across biological kingdoms and the associated biosynthetic pathways, mechanisms, and enzymes are well documented [13]. Basically, the common precursor for biosynthesis of tetrapyrroles is 5-aminolevulinic acid (5-ALA), which can be derived via either the C5 or C4/Shemin pathway with different upstream conversion steps for 5-ALA generation [14]. For post-5-ALA conversion steps, bacteria develop two distinct, i.e., classical (protoporphyrin-dependent; PPD) and non-classical (coproporphyrin-dependent; CPD), branches toward heme biosynthesis [13]. Portions of the PPD and CPD branches might coexist in an organism, leading to different mechanisms/pathways for heme biosynthesis under different environmental conditions and challenges. While bacterium

https://doi.org/10.35534/sbe.2024.10002

Escherichia coli (*E. coli*) primarily utilizes the PPD branch for heme biosynthesis (Figure 1), the simultaneous presence of several enzymes and pathways diverging from the PPD branch offers potential opportunities for biosynthesis of specific porphyrins other than heme, such as uroporphyrin (UP) and coproporphyrin (CP). Herein, we focused on UP for its bio-based production in *E. coli*. Note that UP has potential applications in novel therapeutics and diagnostics, such as photodynamic therapy (PDT) for cancer treatment and antimicrobial therapy [15]. Traditional chemical synthesis of UP requires specific catalysts and involves complicated oxidation steps, making the process intricate and environmentally unfriendly [6]. To date, there has been no report on bio-based production of UP.

In *E. coli*, UP can be an end product in the metabolic branch divergent from the heme biosynthetic pathway at either hydroxymethylbilane (HMB; leading to uroporphyrin I (UP-I)) or uroporphyrinogen III (UPG-III; leading to uroporphyrin III (UP-III)) (Figure 1). Although *E. coli* has the native C5 pathway, it can be metabolically and energetically constrained for 5-ALA generation since this route requires the expression of multiple tightly regulated enzymes, the utilization of ATP and NADPH as limiting cofactors, and the formation of unstable glutamate-1-semialdehyde (GSA) intermediates [16]. To address these limitations in this study, we exploited the Shemin/C4 pathway by heterologous expression of *hemA* from *Rhodobacter sphaeroides* as we have previously developed an effective metabolic strategy [16] to redirect dissimilated carbon flux within the citric acid cycle toward succinyl-CoA, which is a key precursor/moiety to form 5-ALA. Such metabolic strategies were applied to enhance several value-added chemicals derived from succinyl-CoA, including propionate [17], 3-hydroxyvalerate [18], porphobilinogen (PBG) [19], and poly(3-hydroxybutyrate-co-3-hydroxyvalerate) [20].

After 5-ALA formation, two 5-ALA molecules are fused to form PBG by PBG synthase (HemB). Four PBG molecules are subsequently interconnected and cyclized by PBG deaminase (HemC) to form a linear tetrapyrrole HMB. At this point, the pathway can diverge to form either of the two stereoisomers, i.e., UPG-I via autoxidation or UPG-III via uroporphyrinogen III synthase (HemD). Both UPG-I and UPG-III can be spontaneously oxidized to form UP-I and UP-III, respectively, as metabolic end products. Alternatively, UPG-I/III can be enzymatically converted to coproporphyrinogen I/III (CPG-I/III) for subsequent formation of coproporphyrin I/III (CP-I/III) as metabolic end products [21,22].

Modern biotechnologies, such as synthetic biology, metabolic engineering, and genome engineering, have been extensively applied for genetic construction of microbial cell factories [23,24]. However, such bio-based production approaches remain challenging often due to the complex molecular and regulatory mechanisms associated with the engineered genetic and metabolic elements. For effective production of target metabolites, it is critical to implement not only proper metabolic pathways but also optimal tuning of the expression of various pathway genes, particularly those associated with the key conversion step(s) limiting the overall metabolite productivity. In this study, we heterologously implemented the Shemin/C4 pathway in an *E. coli* strain with an enlarged intracellular pool of succinyl-CoA to enhance UP biosynthesis. By exploring different combinations of selective pathway genes for heterologous expression, we were able to characterize individual gene effects and identify key step(s) limiting UP biosynthesis. To further increase the economic feasibility of the developed bioprocess, we used glycerol, which has emerged as a promising carbon source for bio-based production due to its low cost, abundance, and highly reduced nature [25], for cultivation of engineered *E. coli* strains with enhanced UP biosynthesis.

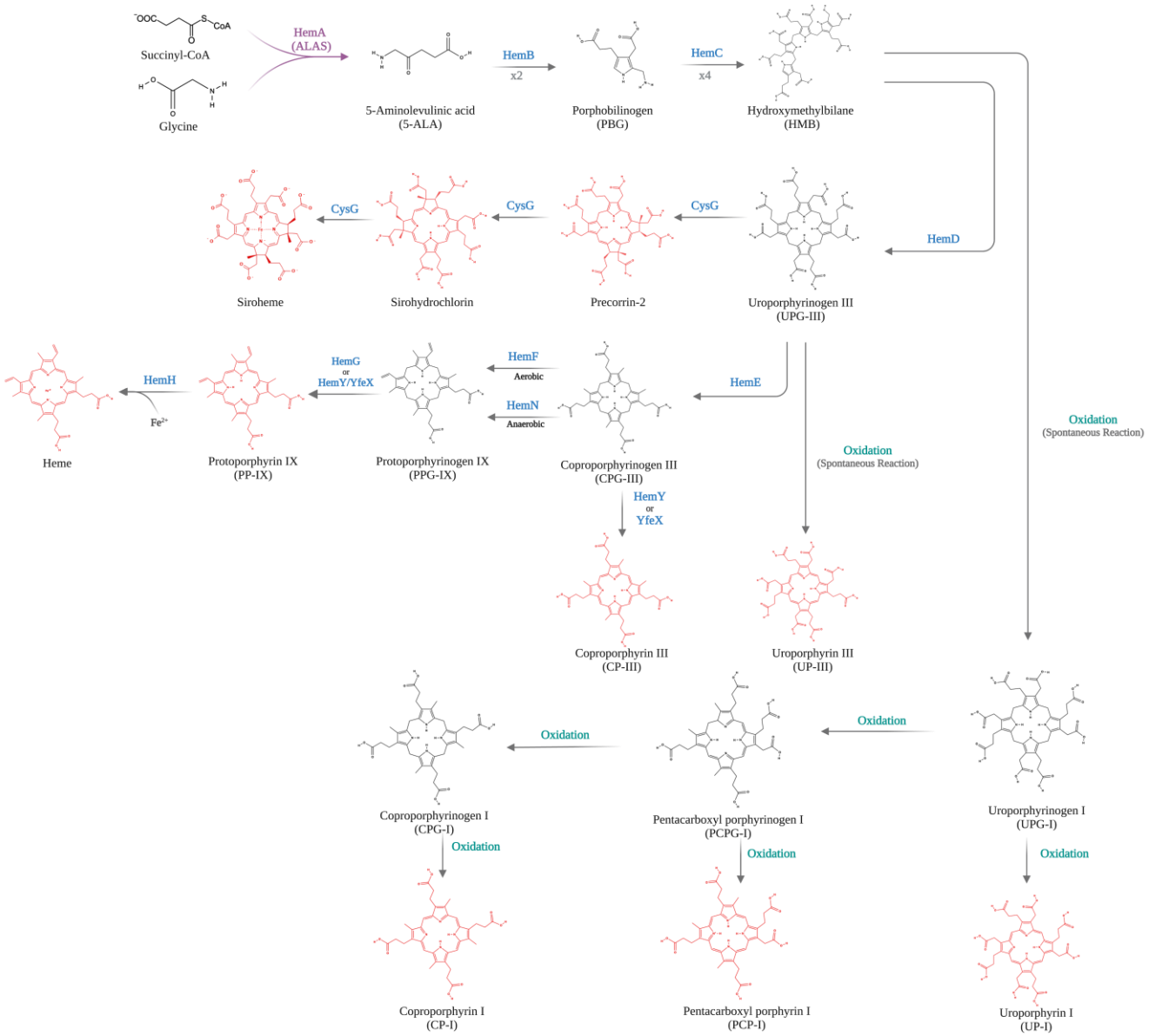

Figure 1. The Shemin/C4 pathway for porphyrin biosynthesis from succinyl-CoA and glycine. Shemin pathway (in violet); Porphyrin biosynthesis (in grey). Pigments (in red); 5-ALA, 5-aminolevulinic acid; CPG-I, coproporphyrinogen I; CPG-III, coproporphyrinogen III; CP-I, coproporphyrin I; CP-III, coproporphyrin III; HMB, Hydroxymethylbilane; HemA, 5-aminolevulinate synthase; HemB, porphobilinogen synthase; HemC, porphobilinogen deaminase; HemD, uroporphyrinogen III synthase; HemE, uroporphyrinogen decarboxylase; HemF, coproporphyrinogen III oxidase; HemG, protoporphyrinogen oxidase; HemH, protoporphyrin ferrochelatase; HemN, oxygen-independent coproporphyrinogen III oxidase; HemY, coproporphyrinogen III oxidase; PBG, porphobilinogen; PCP-I, pentacarboxyl porphyrin I; PCPG-I, pentacarboxyl porphyrinogen I; PP-IX, protoporphyrin IX; PPG-IX, protoporphyrinogen IX; UP-I, uroporphyrin I; UP-III, uroporphyrin III; UPG-I, uroporphyrinogen I; UPG-III, uroporphyrinogen III; YfeX, porphyrinogen peroxidase.

2. Materials and Methods

2.1. Bacterial Strains and Plasmids

The bacterial strains and plasmids utilized in this research are described in Table 1, whereas the primer sequences are provided in Table S1. Genomic DNA from bacterial cells was extracted with the Qiagen Blood & Tissue DNA Isolation Kit (Hilden, Germany). Taq DNA polymerase was obtained from New England Biolabs (Ipswich, MA, USA). All host cells in this study were derived from CPC-Sbm by introducing mutation(s) in the *sdhA* and/or *iclR* genes to direct the carbon flux in the tricarboxylic acid (TCA) cycle toward succinyl-CoA formation ensuring abundant supply of precursors [17]. Note that CPC-Sbm was derived from BW25113 by inactivating the *ldhA* gene [26]. *E. coli* HI-Control 10G (Lucigen, Middleton, WI, USA) was used for molecular cloning. Plasmids were purified using the Qiagen Miniprep kit. DNA sequencing was performed by The Centre for Applied Genomics (TCAG) (Toronto, ON, Canada). Gibson assembly [27] was employed for plasmid construction. All oligonucleotides were synthesized by Integrated DNA Technologies (IDT) (Coralville, IA, USA).

Plasmid pK-hemABCD was first constructed to serve as the template for the other plasmids in this study. The *hemA* gene was amplified by polymerase chain reaction (PCR) from the genomic DNA of *R. sphaeroides* DSM 158 using primers P001/P002. Similarly, *hemB*, *hemC*, and *hemD* genes were amplified from the genomic DNA of *E. coli* MG1655 using primer sets P003/P004, P005/P006, and P007/P008, respectively. The backbone, consisting of p15A ori and P_{trc} with a kanamycin resistance marker, was amplified from a lab-made plasmid using primers P009/P010. Subsequently, these five fragments were Gibson-assembled to form pK-hemABCD. To construct pK-hemA, primers P011/P012 were first phosphorylated and then used to amplify a single fragment from pK-hemABCD as template. The resulting fragment was self-ligated to form pK-hemA. Similarly, a single fragment was amplified from pK-hemABCD with phosphorylated primers P011/P013. This fragment was self-ligated to form pK-hemAB. pK-hemABC was constructed using primer sets P014/P002 and P003/P015 to amplify the backbone and *hemA* in the first fragment and *hemB* and *hemC* in the second fragment. These two fragments were Gibson-assembled to form pK-hemABC. pK-hemABC^{B} was constructed by first amplifying *hemA* and *hemB* as a single fragment from pK-hemABCD using primers P001/P004. Primers P016/P017 were used to amplify *hemC* from the genomic DNA of *Bacillus subtilis* 168. The backbone was amplified using primers P018/P019 from pK-hemABCD. These three fragments were Gibson assembled to form pK-hemABC^{B}. Finally, pK-hemABD was constructed by amplifying *hemA* and *hemB* using primers P001/P004 and amplifying *hemD* along with the backbone using primers P020/P021 and pK-hemABCD as template. These two fragments were Gibson-assembled to form pK-hemABD.

Table 1. Strains and plasmids used in this study.

Name	Description or Relevant Genotype	Source
Host strains		
HI-Control 10G	*mcrA*, Δ(*mrr-hsdRMS-mcrBC*), *endA1*, *recA1*, *ϕ*80*dlacZ*ΔM15, Δ*lacX74*, *araD139*, Δ(*ara leu*)*7697*, *galU*, *galK*, *rpsL* (Str^R), *nupG*, λ^-, *tonA*, Mini-F *lacI*^{q1} ($Gent^R$)	Lucigen
MG1655	K-12; F^-, λ^-, *rph-1*	Lab stock
Bacillus Subtilis 168	Wild type	Lab stock
CPC-Sbm*ΔiclRΔsdhA*	F^-, Δ*(araD-araB)567*, Δ*lacZ4787(::rrnB-3)*, λ^-, *rph-1*, Δ*(rhaD-rhaB)568*, *hsdR514*, Δ*ldhA*, P_{trc}*::sbm* (i.e., with the FRT-P_{trc} cassette replacing the 204-bp upstream of the Sbm operon),Δ*iclR*, Δ*sdhA*	[17]
CPC-Sbm*ΔsdhA*	F^-, Δ*(araD-araB)567*, Δ*lacZ4787(::rrnB-3)*, λ^-, *rph-1*, Δ*(rhaD-rhaB)568*, *hsdR514*, Δ*ldhA*, P_{trc}*::sbm* (i.e., with the FRT-P_{trc} cassette replacing the 204-bp upstream of the Sbm operon), Δ*sdhA*	[17]
DMA	CPC-Sbm*ΔiclRΔsdhA*/pK-hemA	This study
DMB	CPC-Sbm*ΔiclRΔsdhA*/pK-hemAB	This study
DMC	CPC-Sbm*ΔiclRΔsdhA*/pK-hemABC	This study
DMC^{B}	CPC-Sbm*ΔiclRΔsdhA*/pK-hemABC^{B}	This study
DMD	CPC-Sbm*ΔiclRΔsdhA*/pK-hemABD	This study
SMD	CPC-Sbm*ΔsdhA*/pK-hemABD	This study
Plasmids		
pK-hemABCD	p15A ori, Km^R, P_{trc}*::hemABCD*	This study
pK-hemA	p15A ori, Km^R, P_{trc}::*hemA*	This study
pK-hemAB	p15A ori, Km^R, P_{trc}::*hemAB*	This study
pK-hemABC	p15A ori, Km^R, P_{trc}::*hemAB*C	This study
pK-hemABC^{B}	p15A ori, Km^R, P_{trc}::*hemAB*C *-hemC* from *B. subtilis 168-*	This study
pK-hemABD	p15A ori, Km^R, P_{trc}::*hemAB*D	This study

2.2. Media and Bacterial Cell Cultivation

All medium components were obtained from Sigma-Aldrich Co. (St. Louis), except for yeast extract and tryptone, which were obtained from BD Diagnostic Systems (Franklin Lakes). *E. coli* strains were preserved as glycerol stocks at −80 °C and streaked on lysogeny broth (LB; 10 g/L tryptone, 5 g/L yeast extract, and 5 g/L NaCl) agar plates, followed by incubation at 37 °C for 14–16 h.

For bioreactor cultivation, individual single colonies were picked from Luria-Bertani (LB) plates to inoculate 12 mL of super broth (SB) medium (32 g/L tryptone, 20 g/L yeast extract, and 5 g/L NaCl) in a 125 mL conical flask. The culture was incubated at 37 °C and 280 revolutions per min (rpm) using a rotary shaker (New Brunswick Scientific) for 4–6 h and subsequently used as a seed culture to inoculate 220 mL of SB medium at a 2% (*v*/*v*) concentration in a 1 L conical flask. This second seed culture was incubated at 37 °C and 280 rpm for 14–16 h. Cells were harvested by centrifugation at 4500× *g* and 20 °C for 8 min and resuspended in 30 mL of fresh SB medium. The resuspended culture was used to inoculate a stirred-tank bioreactor (CelliGen 115, Eppendorf AG, Hamburg, Germany) with a working volume of 0.8 L at 37 °C and 430 rpm. The semi-defined production medium in the batch bioreactor contained 30.0 g/L glycerol, 0.23 g/L K_2HPO_4, 0.51 g/L NH_4Cl, 49.8 mg/L $MgCl_2$, 48.1 mg/L K_2SO_4, 1.52 mg/L $FeSO_4$, 0.055 mg/L $CaCl_2$,

2.93 g/L NaCl, 0.72 g/L tricine, 10.0 g/L yeast extract, 10.0 mM $NaHCO_3$, and 1.0 mL/L trace elements (2.86 g/L H_3BO_3, 1.81 g/L $MnCl_2 \cdot 4H_2O$, 0.222 g/L $ZnSO_4 \cdot 7H_2O$, 0.39 g/L $Na_2MoO_4 \cdot 2H_2O$, 79.0 μg/L $CuSO_4 \cdot 5H_2O$, 49.4 μg/L $Co(NO_3)_2 \cdot 6H_2O$) [28], supplemented with 0.05 mM isopropyl β-D-1-thiogalactopyranoside (IPTG). To avoid glycine limitation during the cultivation, 2.0 g of glycine was supplemented into the bioreactor ~30 h after the inoculation.

Aeration Level I (AL-I) with an aerobic condition was maintained by continuously purging the air into the bulk culture at 1 volume of air per volume of liquid per min (vvm). Aeration Level II (AL-II) was maintained by initially purging the air into the bulk culture at 1 vvm for the first 30 h, followed by switching to a microaerobic condition by purging the air into the headspace at 0.1 vvm. Aeration Level III (AL-III) was similar to AL-II during the initial aerobic phase; but followed by switching to an anaerobic condition by purging nitrogen (N_2) into the headspace. The pH of the bioreactor culture was maintained at 7.0 ± 0.1 using 3.0 M NH_4OH and 3.0 M H_3PO_4.

2.3. Analysis

Culture samples were appropriately diluted using a 0.15 M saline solution to measure cell density in OD_{600} with a spectrophotometer (DU520, Beckman Coulter, Fullerton, CA, USA). All culture samples were washed one time with 0.15 M saline solution prior to OD_{600} absorbance measurement. To prepare cell-free medium, culture samples were centrifuged at 17,000× *g* for 1 min and then filter sterilized using a 0.2 μm syringe filter. Extracellular metabolites and glycerol were analyzed by high-performance liquid chromatography (HPLC; LC-10AT; Shimadzu, Kyoto, Japan) with a refractive index detector (RID; RID-10A; Shimadzu) and a chromatographic column (Aminex HPX-87H; Bio-Rad Laboratories, CA, USA). The HPLC column temperature was maintained at 35 °C and the mobile phase was 5.0 mM H_2SO_4 (pH 2) running at 0.6 ml/min. The RID signal was analyzed by a data processing software (Clarity Lite, DataApex, Prague, Czech Republic). The concentrations of 5-ALA and PBG in the cell-free medium were determined using an assay with a modified Ehrlich's reagent [29]. Porphyrins were analyzed using an HPLC (2690 separation module, Waters™) with a photodiode array (PDA; 2996 PDA detector, Waters™) detector and a chromatographic column (Chromolith® HighResolution RP-18 endcapped, Supelco, Darmstadt, Germany). The UV absorbance was measured at 400 nm and the signal was analyzed using a data processing software (Empower 3, Waters™, Milford, USA). A previously described mobile-phase system was employed [10] with minor modifications. Briefly, the mobile phase consisted of two solvent mixtures: solvent A (7.7 g/L ammonium acetate, 125.0 mL/L acetonitrile, adjusted to pH 5.17 with glacial acetic acid) and solvent B (a methanol-glacial acetic acid mixture with a volume ratio at 10:1). The flow rate of the mobile phase was 1 mL/min. An isocratic elution step was used with 100% solvent A for 5 min, followed by a linear gradient from 0 to 100% solvent B over 30 min, and further followed by 100% solvent B for 5 min. The column temperature was maintained at 45 °C. The percentage yield of UP was calculated as the mole ratio of the produced UP to the theoretical maximum UP production based on the consumed glycerol, assuming a one-to-sixteen molar ratio (i.e., one mole UP produced per sixteen moles of glycerol consumed). Note that eight moles of succinyl-CoA (derived from 16 moles of glycerol) and eight moles of glycine are needed to generate one mole UP.

3. Results

3.1. Implementation of the Shemin/C4 Pathway for UP Biosynthesis

We implemented the Shemin/C4 pathway by heterologous expression of *hemA* from *R. sphaeroides* in CPC-SbmΔ*iclR*Δ*sdhA*, resulting in DMA strain. For abundant supply of precursors, the dissimilated carbon flux in the TCA cycle was directed toward succinyl-CoA under aerobic conditions based on the double mutation Δ*iclR*Δ*sdhA* [16]. We also supplemented all the cultures with 2.0 g/L glycine to ensure that the culture performance was not limited by glycine supply. Both DMA and the control strain (CPC-SbmΔ*iclR*Δ*sdhA*) were cultivated in a batch bioreactor under aerobic conditions. Unless otherwise noted, all titers reported here are associated with the last cultivation samples, and we calculated the percentage yield as the ratio of the actual yield of the produced metabolite to the theoretical yield based on consumed glycerol. Compared to the control strain with relatively fast cell growth and glycerol consumption, DMA had a much lower biomass yield with substantial growth inhibition and acetogenesis (Figures 2A and 3A). Note that DMA generated much higher levels of 5-ALA, which peaked at 215.0 mg/L (22.6 mg/OD_{600}/L) at 71 h, and PBG, which peaked at 150.0 mg/L (15.9 mg/OD_{600}/L) (Figures 2B and 3B) with significant pigmentation (Figure 3D), producing 55.3 mg/L (0.32% yield) and 41.9 mg/L (0.25% yield) of UP-I and UP-III, respectively (Figure 3C). The results suggest that the implemented Shemin/C4 pathway was functional with an enhanced carbon flux redirected from the TCA cycle for UP biosynthesis in DMA.

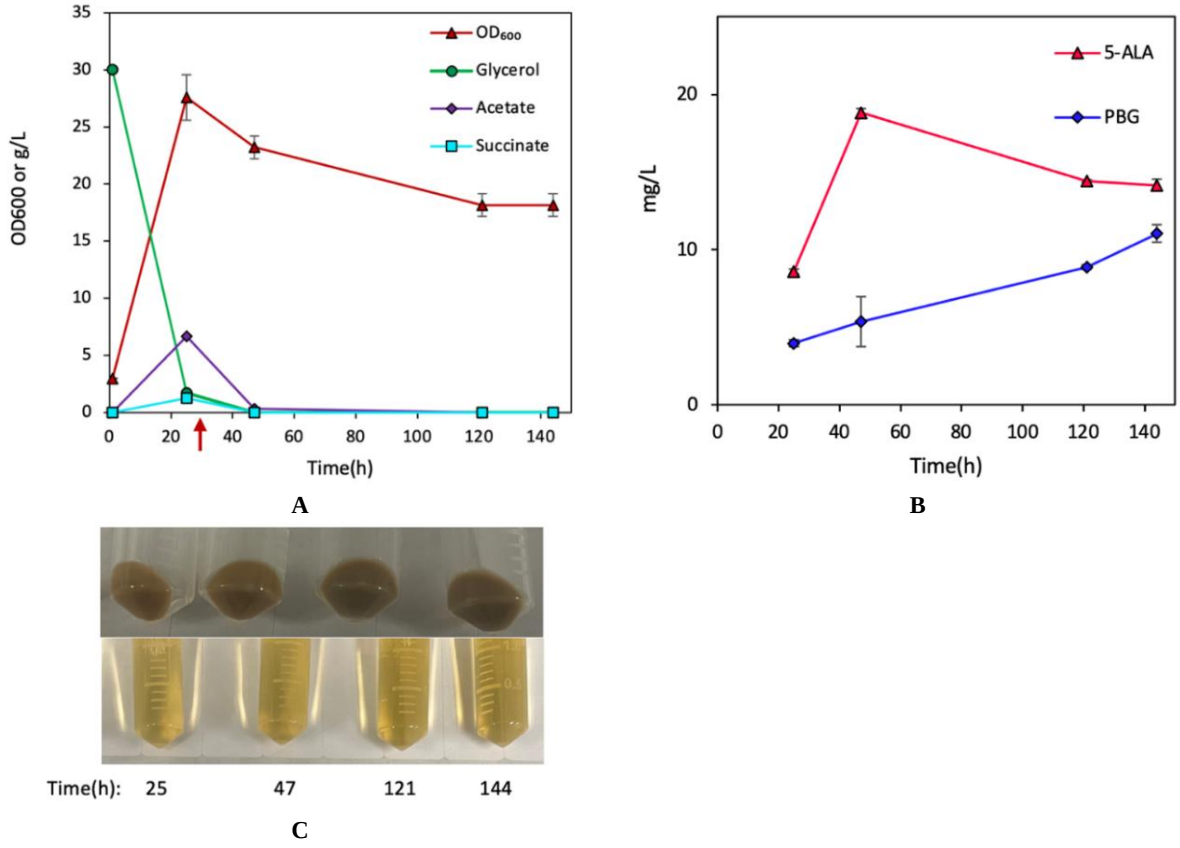

Figure 2. Bioreactor cultivation of the control strain CPC-SbmΔ*iclR*Δ*sdhA*. Time profiles of (**A**) cell density (OD_{600}), glycerol consumption, and acetate/succinate production, (**B**) 5-ALA and PBG biosynthesis, and (**C**) Image of CFM and cell paste samples at different time points. The red arrow shows glycine supplementation. All values are reported as means ± SD (*n* = 2).

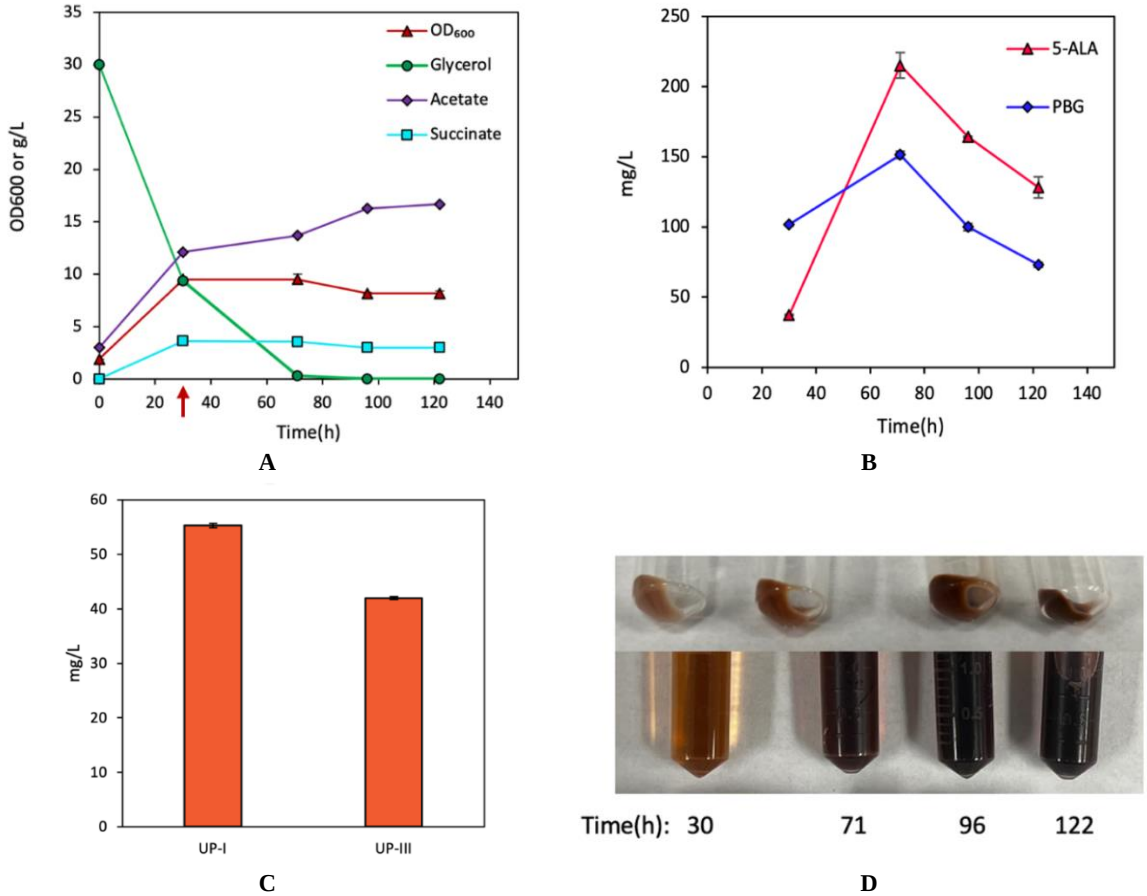

Figure 3. Bioreactor cultivation of DMA for porphyrin biosynthesis. Time profiles of (**A**) cell density (OD_{600}), glycerol consumption, and acetate/succinate formation, (**B**) 5-ALA and PBG biosynthesis, and (**C**) UP biosynthesis. (**D**) Image of CFM and cell paste samples at different time points. The red arrow shows glycine supplementation. All values are reported as means ± SD (*n* = 2).

3.2. Effects of the Native HemB on UP Biosynthesis

Next, to investigate the effects of native HemB on UP biosynthesis, we derived another UP-producing strain DMB by coexpression of *hemB* from *E. coli* and *hemA* from *R. sphaeroides*. Effective coexpression of *hemA* and *hemB* was achieved from a single operon, which was expressed from the strong *trc* promoter and included strong ribosomal binding sites (RBS) for each gene in plasmid pK-hemAB. Compared to DMA, aerobic cultivation of DMB strain showed a slightly better biomass yield with a slower glycerol consumption and a similar level of acetogenesis (Figure 4A). However, DMB produced much higher 5-ALA and PBG, with peak levels of 304.3 mg/L (20.9 mg/OD_{600}/L) and 1995.0 mg/L (193.0 mg/OD_{600}/L), respectively (Figure 4B). Additionally, the DMB cultivation had more intensified pigmentation, producing 555.3 mg/L (3.7% yield) and 346.6 mg/L (2.3% yield) of UP-I and UP-III, respectively (Figure 4C,D). The results suggest that, in addition to 5-ALA, the formation of PBG could be another key step limiting the overall UP biosynthesis in *E. coli*.

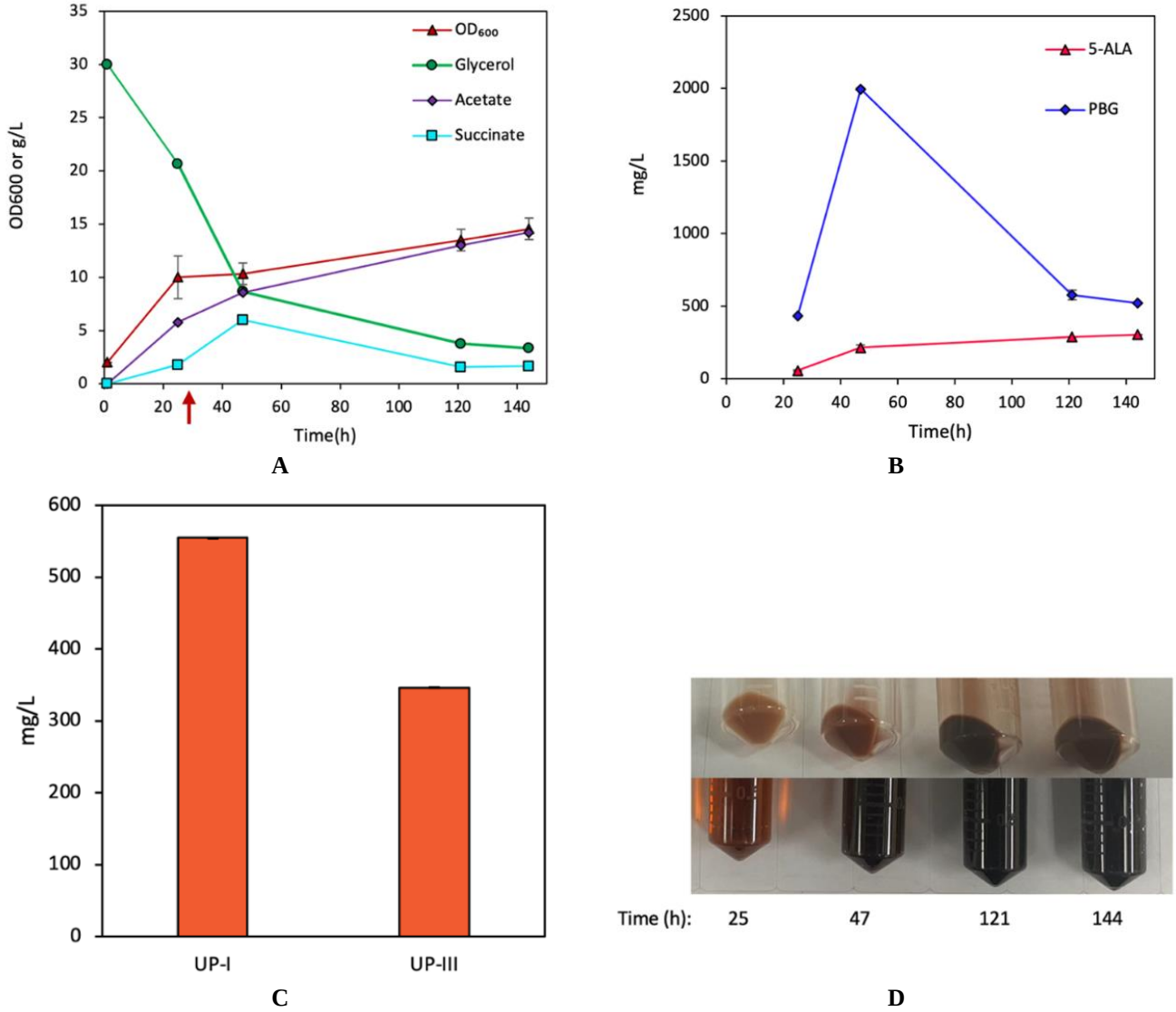

Figure 4. Bioreactor cultivation of DMB for porphyrin biosynthesis. Time profiles of (**A**) cell density (OD_{600}), glycerol consumption, and acetate/succinate formation, (**B**) 5-ALA and PBG biosynthesis, and (**C**) UP biosynthesis. (**D**) Image of CFM and cell paste samples at different time points. The red arrow shows glycine supplementation. All values are reported as means±SD (n = 2).

3.3. Effects of HemC from E. coli and B. Subtilis on UP Biosynthesis

Next, we investigated the effects of the native HemC on UP biosynthesis. To do this, we derived another strain, DMC, by coexpression of the native *hemB* and *hemC* from *E. coli* and *hemA* from *R. sphaeroides*. Similar to pK-hemAB, we included all three genes in an operon as *hemABC* regulated by the common *trc* promoter with an individual strong RBS for each gene. Surprisingly, cultivation of the DMC strain exhibited no pigmentation (Figure 5C), similar to the control strain (CPC-SbmΔ*iclR*Δ*sdhA*) though the culture grew normally with a rapid glycerol consumption rate and minimal acetogenesis (Figure 5A). Notably, the low levels of 5-ALA and PBG for DMC, only up to 14.0 mg/L (0.84 mg/OD_{600}/L) and 11.0 mg/L (0.67 mg/OD_{600}/L), respectively (Figure 5B), were also similar to those of the control strain. These findings suggest that the overexpression of the native *hemC* gene potentially disrupted the metabolic activity of the Shemin/C4 pathway.

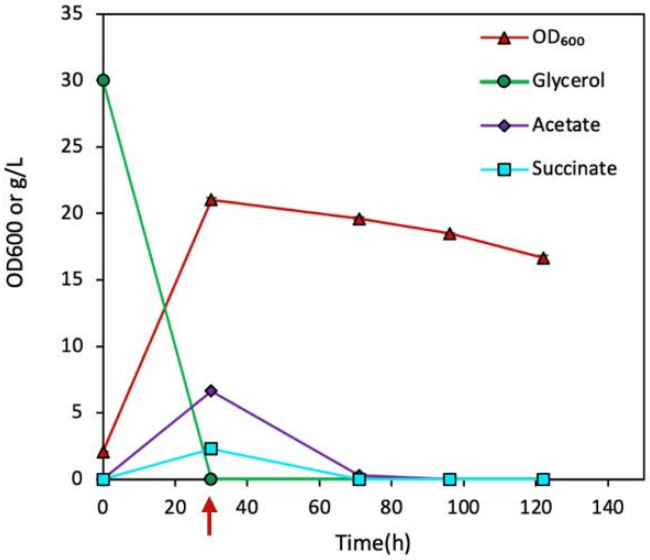

A

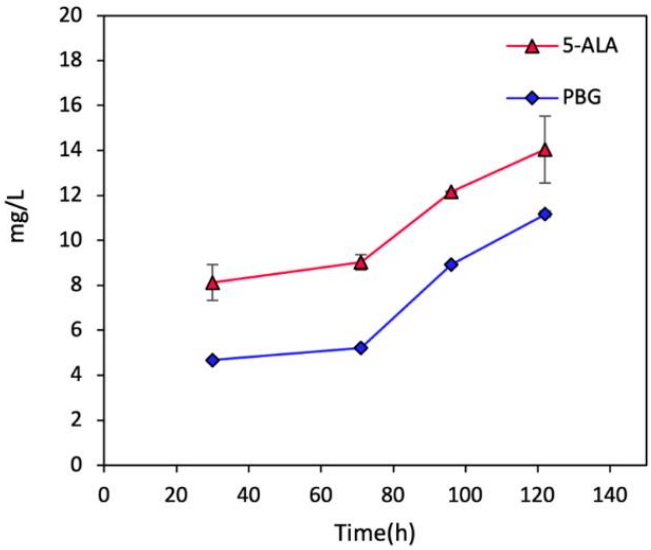

B

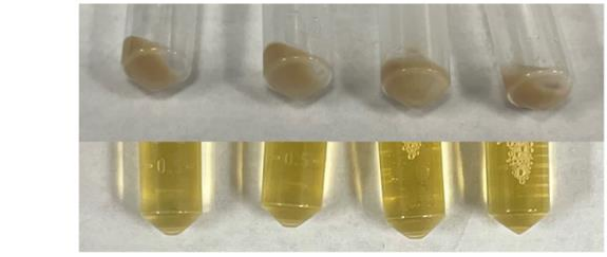

C

Figure 5. Bioreactor cultivation of DMC for porphyrin biosynthesis. Time profiles of (**A**) cell density (OD_{600}), glycerol consumption, and acetate/succinate formation, (**B**) 5-ALA and PBG biosynthesis, and (**C**) Image of CFM and cell paste samples at different time points. The red arrow shows glycine supplementation. All values are reported as means±SD (*n* = 2).

In parallel, we examined the effects of HemC from B. subtilis on UP biosynthesis. To do this, we generated pK-hemABC^{B} with the same plasmid design as pK-hemABC except that the native *hemC* was replaced by *hemC* from *B. subtilis*. Unlike DMC strain, cultivation of the resulting strain DMC^{B} displayed a significant pigmentation (Figure 6D) with partially retarded cell growth (similar to DMB) and minimal acetogenesis (Figure 6A). Furthermore, DMC^{B} exhibited increased production of 5-ALA and PBG in comparison to DMC, with peak levels being 81.2 mg/L (5.25 mg/OD_{600}/L) and 108.3 mg/L (7.0 mg/OD_{600}/L), respectively (Figure 6B). However, the significant PBG accumulation (observed in DMB) was not observed in DMC^{B}, suggesting that the expressed HemC from *B. subtilis* effectively converted PBG to HMB in the early cultivation stage (Figures 4B and 6B). Nevertheless, DMC^{B} produced UP-I and UP-III significantly lower than DMB, with peak levels of 200.4 mg/L (1.18% yield) and 135.0 mg/L (0.8% yield), respectively (Figure 6C). These observations further suggest adverse effects of increasing *hemC* expression on UP biosynthesis.

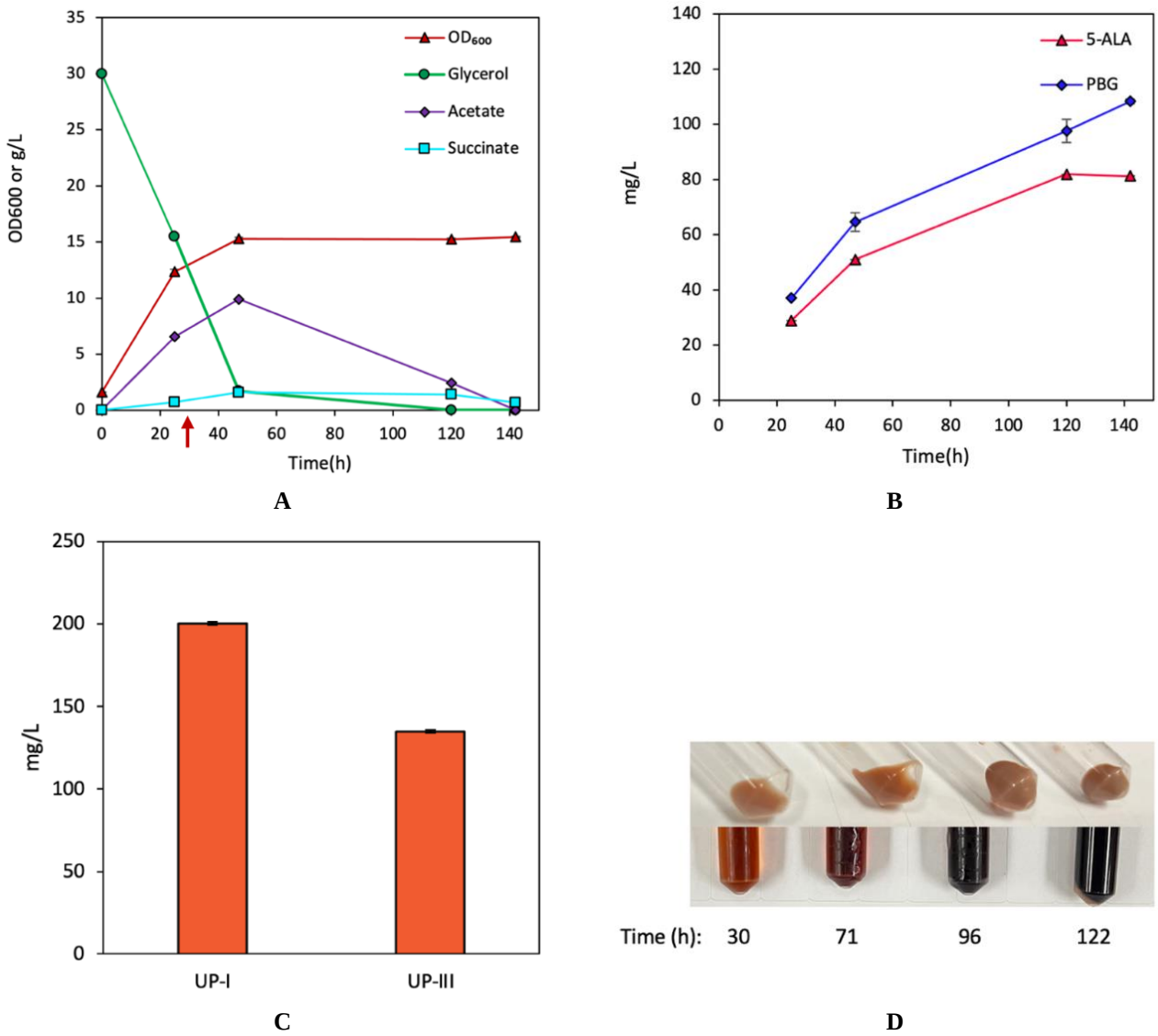

Figure 6. Bioreactor cultivation of DMC^{B} for porphyrin biosynthesis. Time profiles of (**A**) cell density (OD_{600}), glycerol consumption, and acetate/succinate formation, (**B**) 5-ALA and PBG biosynthesis, and (**C**) UP biosynthesis. (**D**) Image of CFM and cell paste samples at different time points. The red arrow shows glycine supplementation. All values are reported as means ± SD (n = 2).

3.4. Effects of the Native HemD on UP Biosynthesis

To investigate the effects of the native HemD on UP biosynthesis, we derived a plasmid pK-hemABD for overexpressing the native *hemB* and *hemD* with *hemA* from *R. sphaeroides* in CPC-SbmΔ*iclR*Δ*sdhA* and CPC-SbmΔ*sdhA*, resulting in DMD and SMD strains, respectively. We excluded *hemC* as its overexpression was detrimental to the Shemin/C4 pathway for porphyrin biosynthesis. DMD had a similar growth pattern and glycerol consumption rate to DMB during aerobic cultivation and significant acetogenesis (Figure 7A). Notably, DMD produced high levels of 5-ALA and PBG, peaking at 196.0 mg/L (18.2 mg/OD_{600}/L) and 1117.0 mg/L (83.16 mg/OD_{600}/L) at 57 h, respectively (Figure 7B). Similar to DMB with significant pigmentation, DMD produced a total UP of 826.45 mg/L (comprising 538.9 mg/L UP-I and 287.5 mg/L UP-III, at 3.18% and 1.7% yields, respectively) (Figure 7C,D). Note that the distribution of UP-I and UP-III in DMD resembled that of DMB, suggesting that *hemD* overexpression did not enhance the metabolic flux toward the classical pathway, suggesting that conversion of HMB via the autoxidation reaction was more effective than the enzymatic reaction by HemD even upon *hemD* overexpression.

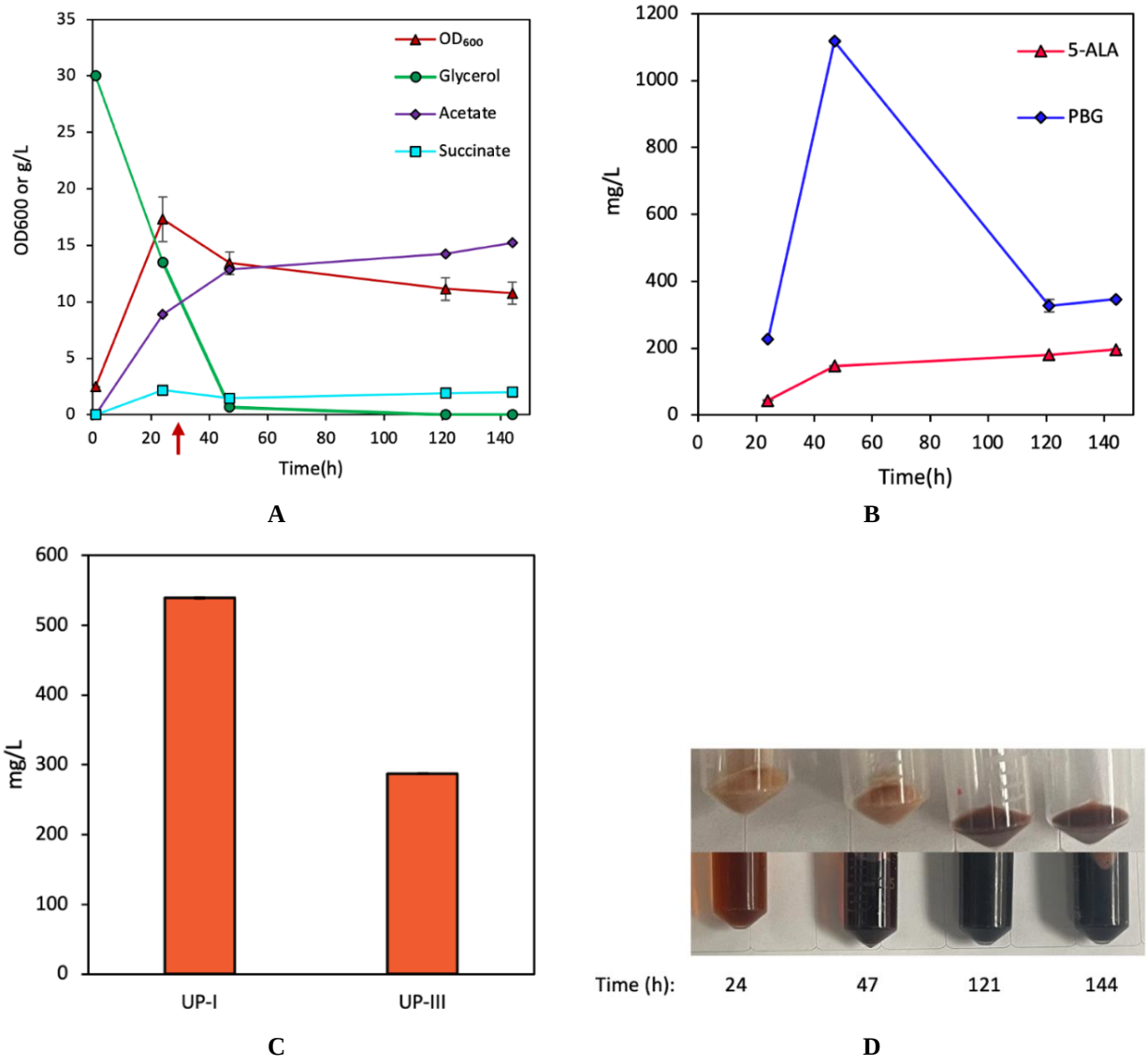

Figure 7. Bioreactor cultivation of DMD for porphyrin biosynthesis. Time profiles of (**A**) cell density (OD_{600}), glycerol consumption, and acetate/succinate formation, (**B**) 5-ALA and PBG biosynthesis, and (**C**) UP biosynthesis. (**D**) Image of CFM and cell paste samples at different time points. The red arrow shows glycine supplementation. All values are reported as means±SD (*n* = 2).

To investigate the effects of oxygenic condition on the autoxidation (converting HMB to UP-I), we conducted *hemD* overexpression in SMD under lower oxygenic conditions (i.e., AM-II/microaerobic and AM-III/anaerobic). While reducing oxygenic condition for SMD did not seriously affect cell growth and glycerol dissimilation compared to aerobic cultivation of DMD (Figures 8A and 9A), such environmental manipulation impacted metabolic activity associated with UP biosynthesis. Compared to DMD, SMD only produced 314.9 mg/L UP-I (1.86% yield) and 171.7 mg/L UP-III (1.01% yield) under AM-II, and 37.1 mg/L (0.22% yield) UP-I, 4.78 mg/L (0.02% yield) UP-III, and 19.6 mg/L CP-III (0.14% yield) under AM-III with much lower levels of 5-ALA and PBG (Figures 8B,C and 9B,C). These results suggest that reducing the oxygenic condition impacted both the autoxidation and enzymatic reaction catalyzed by HemD for UP biosynthesis.

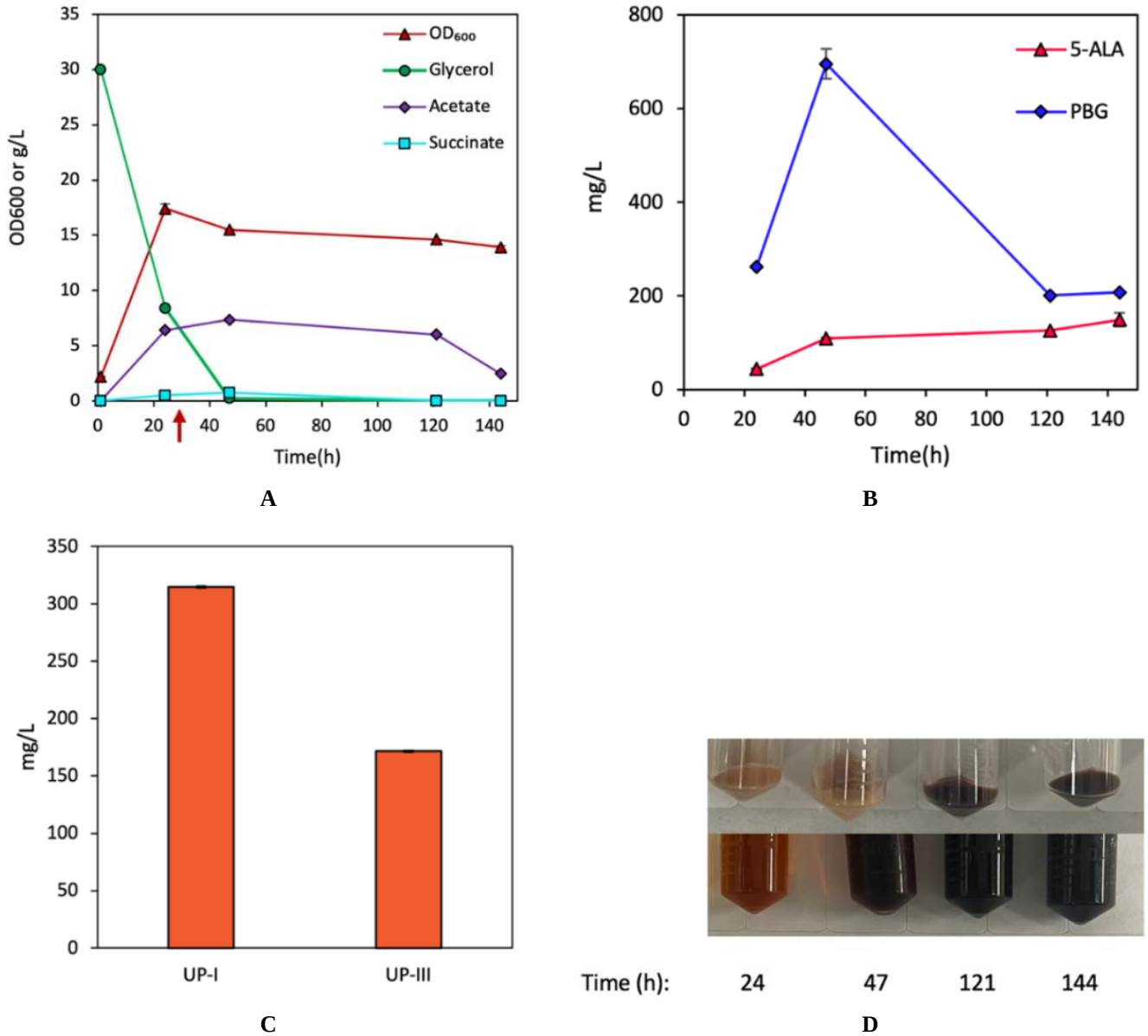

Figure 8. Bioreactor cultivation of SMD for porphyrin biosynthesis under AM-II condition. Time profiles of (**A**) cell density (OD_{600}), glycerol consumption, and acetate/succinate formation, (**B**) 5-ALA and PBG biosynthesis, and (**C**) UP biosynthesis. (**D**) Image of CFM and cell paste samples at different time points. The red arrow shows glycine supplementation. All values are reported as means±SD (n = 2).

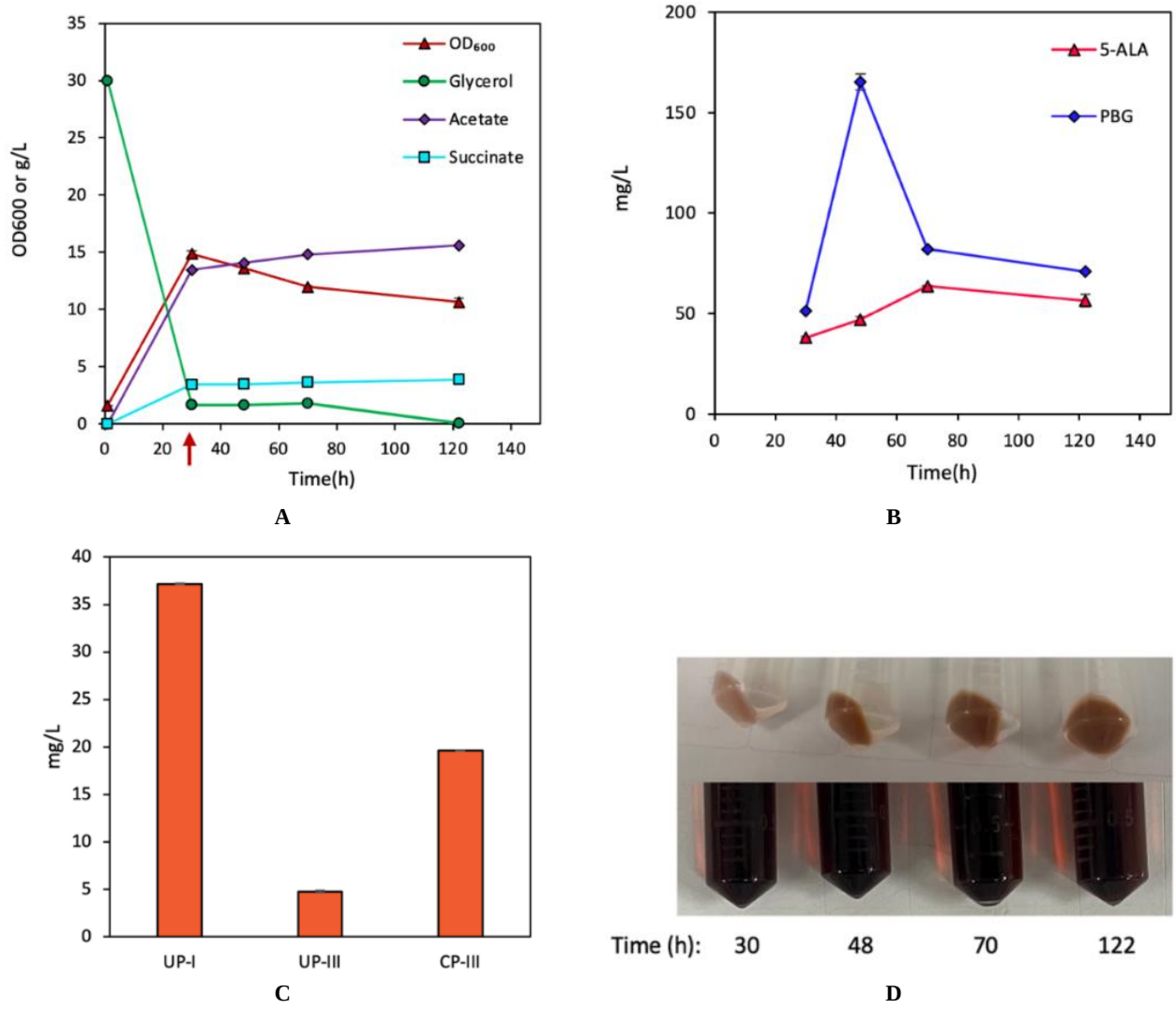

Figure 9. Bioreactor cultivation of SMD for porphyrin biosynthesis under AM-III condition. Time profiles of (**A**) cell density (OD_{600}), glycerol consumption, and acetate/succinate formation, (**B**) 5-ALA and PBG biosynthesis, and (**C**) UP biosynthesis. (**D**) Image of CFM and cell paste samples at different time points. The red arrow shows glycine supplementation. All values are reported as means±SD (n = 2).

4. Discussion

In this study, we enhanced the biosynthesis of UP in *E. coli* via the Shemin/C4 pathway with a redirected carbon flux from the TCA cycle. Note that most of the heterologously synthesized UP was secreted extracellularly with minimal physiological impact on the producing cells, suggesting the bioprocess feasibility for large-scale production of this porphyrin. Compared to the control strain CPC-SbmΔ*iclR*Δ*sdhA*, heterologous expression of *hemA* resulted in high levels of 5-ALA and PBG in DMA with significant culture pigmentation and UP formation, suggesting that the overall UP biosynthesis in DMA was limited by step(s) after 5-ALA formation under this genetic background. The implementation of the Shemin/C4 pathway also resulted in significant acetogenesis, which reduced the available carbon for UP biosynthesis and impacted cell growth/physiology, similar to previous observations [16,19]. The significant pigmentation exhibited by the DMA culture with notable UP formation suggests that *hemC* was actively expressed in this strain. Additionally, the higher production of UP-I than UP-III in DMA indicates a preference for the autoxidation of HMB (under aerobic conditions) over the enzymatic conversion by HemD. In addition, the autoxidation for conversion of UPG-I/III to UP-I/III appears to be effective as well such that both UP-I and UP-III can be metabolic end products extracellularly secreted.

Compared to DMA, heterologous expression of the native *hemB* along with *hemA* in DMB resulted in significant PBG accumulation with enhanced pigmentation and UP biosynthesis. The synergistic catalytic effects of HemA and HemB suggest that PBG formation was another potential step limiting UP biosynthesis, in addition to the previously identified one of 5-ALA formation. The significant culture pigmentation in DMB (and DMA) suggests that the genomic

hemC was actively expressed and the conversion from PBG to HMB was rather effective. Similar to DMA, the relatively higher titer of UP-I than UP-III in DMB suggests that the autoxidation was favored over the enzymatic conversion by HemD, presumably due to aerobic cultivation conditions.

The HemC-mediated conversion of PBG to HMB, which is a critical step to form the initial tetrapyrrole structure, was effective in DMA and DMB based on the level of culture pigmentation, implying that the native genomic *hemC* was actively expressed. It was documented that HemC normally remains stable and abundant in *E. coli* [30]. In a previous study, the expression of *hemC* had to be repressed (via CRISPRi) in order to overproduce PBG, also suggesting a relatively high level of expression of native genomic *hemC* in *E. coli* [19]. Nevertheless, it was surprising to see that heterologous expression of the native *hemC* completely disrupted the metabolic activity of the Shemin/C4 pathway in DMC. Note that the lack of culture pigmentation and low levels of 5-ALA and PBG (i.e., less than 20.0 mg/L), which were comparable to those of the control strain, suggest that HemA was somehow inactivated (presumably by overexpression of the native *hemC*) in DMC. Though the Shemin/C4 pathway remained active upon heterologous expression of *B. subtilis hemC* in DMC^B, UP biosynthesis was negatively impacted. Further research is required to identify the underlying cause of these *hemC* effects.

Our results showed that conversion of HMB to UPG-I via autoxidation was much more effective than the enzymatic conversion to UPG-III by HemD. Overexpression of *hemD* neither increased the overall UP biosynthesis nor the selectivity of HBM conversion to UPG-III. The results suggest that the overall UP biosynthesis was not limited by the step of HMB conversion. Reducing the oxygenic condition, which presumably retards autoxidation, only decreased the overall UP biosynthesis without significantly affecting the selectivity of HBM conversion to UPG-III. Such effective autoxidation for HBM conversion to UPG-I presented major challenges for biosynthesis of downstream porphyrins derived from UPG-III, such as CP, PP-IX, and heme, in *E. coli*. Interestingly, HMB conversion to UPG-III appeared to be enhanced by overexpression of *hemE* (data not shown), even without coexpression of *hemD*. While conversion of UPG-III to UP-III via autoxidation was more effective than conversion to CPG-III via HemE under aerobic conditions, reducing the oxygenic conditions appeared to reverse such conversion preference, leading to formation of CP-III more than UP-III.

Metabolically, structural linking of four molecules of PBG (to form the linear tetrapyrrole of HMB) and subsequent cyclization of HMB (to form either UPG-I or UPG-III) are critical for porphyrin biosynthesis, which can be observable by culture pigmentation. Apparently, both the two conversion steps were effective in *E. coli* based on the levels of culture pigmentation and UP biosynthesis in DMA and DMB, suggesting that genomic expression of *hemC* and *hemD* were abundant and active even under the conditions for enhanced UP biosynthesis. Heterologous overexpression of *hemD* did not enhance the overall UP biosynthesis, whereas heterologous overexpression of *hemC* completely disrupted the metabolic activity of the Shemin/C4 pathway (specifically the HemA-catalytical step for 5-ALA formation) with no UP biosynthesis. Our results demonstrated the importance of optimal tuning of the expression of various enzymes involved in the Shemin/C4 pathway for enhanced UP biosynthesis.

Our study presents valuable insights into UP biosynthesis via the Shemin/C4 pathway in *E. coli*, demonstrating the feasibility of large-scale production. However, several areas offer potential for future research: Investigating the unexpected effects of HemC overexpression on HemA catalysis could provide valuable understanding of the heme pathway. Additionally, exploring strategies to avoid the autooxidation pathway might prevent the formation of unexpected byproducts, enhancing the efficiency of the biosynthesis process. Further investigation into the specific preferences of autoxidation versus enzymatic conversion pathways for HMB conversion would facilitate harnessing these pathways for targeted porphyrin biosynthesis.

Supplementary Materials

The following supporting information can be found at: https://www.sciepublish.com/article/pii/129.

Author Contributions

Conceptualization, B.A. and C.P.C.; Methodology, B.A. and A.W.; Validation, Y.L. and C.P.C.; Formal Analysis, B.A.; Investigation, B.A.; Data Curation, B.A.; Writing – Review & Editing, B.A. and C.P.C.; Supervision, C.P.C.; Funding Acquisition, M.M.Y. and C.P.C.

Ethics Statement

Not applicable.

Informed Consent Statement

Not applicable.

Funding

This research was funded by Natural Sciences and Engineering Research Council (NSERC) grant number RGPIN-2019-04611. We acknowledge technical assistance in bacterial cultivation from Mr. M. Zim.

Declaration of Competing Interest

The authors declare no conflict of interest.

References

1. Cook LP, Brewer G, Wong-Ng W. Structural Aspects of Porphyrins for Functional Materials Applications. *Crystals* **2017**, *7*, 223.
2. Shi Y, Zhang F, Linhardt R. Porphyrin-based compounds and their applications in materials and medicine. *Dyes Pigm.* **2021**, *188*, 109136.
3. Zhou Q, Yamada A, Feng Q, Hoskins A, Dunietz BD, Lewis KM. Modification of Molecular Conductance by in Situ Deprotection of Thiol-Based Porphyrin. *ACS Appl. Mater. Interfaces* **2017**, *9*, 15901–15906.
4. Mondal S, Pain T, Sahu K, Kar S. Large-Scale Green Synthesis of Porphyrins. *ACS Omega* **2021**, *6*, 22922–22936.
5. Hiroto S, Miyake Y, Shinokubo H. Synthesis and Functionalization of Porphyrins through Organometallic Methodologies. *Chem. Rev.* **2017**, *117*, 2910–3043.
6. Macdonald SF, Stedman RJ. The Synthesis of Uroporphyrin I. *J. Am. Chem. Soc.* **1953**, *75*, 3040–3041.
7. Rebeiz CA, Haidar MA, Yaghi M. Porphyrin biosynthesis in cell-free homogenates from higher plants. *Plant Physiol.* **1970**, *46*, 543–549.
8. Goldberg A, Rimington C. Experimentally produced porphyria in animals. *Proc. R. Soc. Lond. B Biol. Sci.* **1955**, *143*, 257–279.
9. Hassner A, Namboothiri I. MACDONALD Porphyrin Synthesis to MYERS–SAITO Cycloaromatization. In *Organic Syntheses Based on Name Reactions (Third Edition)*; Elsevier: Amsterdam, The Netherlands; 2012, pp. 297–333.
10. Kwon SJ, de Boer AL, Petri R, Schmidt-Dannert C. High-Level Production of Porphyrins in Metabolically Engineered *Escherichia coli*: Systematic Extension of a Pathway Assembled from Overexpressed Genes Involved in Heme Biosynthesis. *Appl. Environ. Microbiol.* **2003**, *69*, 4875–4883.
11. Moulin M, Smith A. Regulation of tetrapyrrole biosynthesis in higher plants. *Biochem. Soc. Trans.* **2005**, *33*, 737–742.
12. Wu L, Moteki T, Gokhale AA, Flaherty DW, Toste FD. Production of Fuels and Chemicals from Biomass: Condensation Reactions and Beyond. *Chem* **2016**, *1*, 32–58.
13. Kořený L, Oborník M, Horáková E, Waller RF, Lukeš J. The convoluted history of haem biosynthesis. *Biol. Rev.* **2022**, *97*, 141–162.
14. Jiang M, Hong K, Mao Y, Ma H, Chen T, Wang Z. Natural 5-Aminolevulinic Acid: Sources, Biosynthesis, Detection and Applications. *Front. Bioeng. Biotechnol.* **2022**, *10*, 841443.
15. Sharma R, Viana SM, Ng DKP, Kolli BK, Chang KP, de Oliveira CI. Photodynamic inactivation of Leishmania braziliensis doubly sensitized with uroporphyrin and diamino-phthalocyanine activates effector functions of macrophages in vitro. *Sci. Rep.* **2020**, *10*, 17065.
16. Miscevic D, Mao JY, Kefale T, Abedi D, Moo-Young M, Perry Chou C. Strain engineering for high-level 5-aminolevulinic acid production in *Escherichia coli. Biotechnol. Bioeng.* **2021**, *118*, 30–42.
17. Miscevic D, Mao JY, Moo-Young M, Chou CP. High-level heterologous production of propionate in engineered *Escherichia coli*. *Biotechnol. Bioeng.* **2020**, *117*, 1304–1315.
18. Miscevic D, Mao JY, Kefale T, Abedi D, Huang CC, Moo-Young M, et al. Integrated strain engineering and bioprocessing strategies for high-level bio-based production of 3-hydroxyvalerate in *Escherichia coli. Appl. Microbiol. Biotechnol.* **2020**, *104*, 5259–5272.
19. Lall D, Miscevic D, Bruder M, Westbrook A, Aucoin M, Moo-Young M, et al. Strain engineering and bioprocessing strategies for biobased production of porphobilinogen in *Escherichia coli*. *Bioresour. Bioprocess* **2021**, *8*, 122.
20. Miscevic D, Mao JY, Mozell B, Srirangan K, Abedi D, Moo-Young M, et al. Bio-based production of poly (3-hydroxybutyrate-co-3-hydroxyvalerate) with modulated monomeric fraction in *Escherichia coli*. *Appl. Microbiol. Biotechnol.* **2021**, *105*, 1435–1446.

21. Zhang J, Kang Z, Chen J, Du G. Optimization of the heme biosynthesis pathway for the production of 5-aminolevulinic acid in *Escherichia coli*. *Sci. Rep.* **2015**, *5*, 8584.
22. Zappa S, Li K, Bauer CE. The Tetrapyrrole Biosynthetic Pathway and Its Regulation in Rhodobacter capsulatus; In *Recent Advances in Phototrophic Prokaryotes*; Springer: New York, NY, USA. 2010; pp. 229–250.
23. Davy AM, Kildegaard HF, Andersen MR. Cell Factory Engineering. *Cell Syst.* **2017**, *4*, 262–275.
24. Mcarthur GH, Fong SS. Toward Engineering Synthetic Microbial Metabolism. *J. Biomed. Biotechnol.* **2010**, *2010*, 1–10.
25. Westbrook AW, Miscevic D, Kilpatrick S, Bruder MR, Moo-Young M, Chou CP. Strain engineering for microbial production of value-added chemicals and fuels from glycerol. *Biotechnol. Adv.* **2019**, *37*, 538–568.
26. Srirangan K, Liu X, Westbrook A, Akawi L, Pyne ME, Moo-Young M, et al. Biochemical, genetic, and metabolic engineering strategies to enhance coproduction of 1-propanol and ethanol in engineered *Escherichia coli*. *Appl. Microbiol. Biotechnol.* **2014**, *98*, 9499–9515.
27. Gibson DG, Young L, Chuang RY, Venter JC, Hutchison CA 3rd, Smith HO. Enzymatic assembly of DNA molecules up to several hundred kilobases. *Nat. Methods* **2009**, *6*, 343–345.
28. Neidhardt FC, Bloch PL, Smith DF. Culture medium for enterobacteria. *J. Bacteriol.* **1974**, *119*, 736–747.
29. Mauzerall D, Granick S. The Occurrence and Determination of δ-Aminolevulinic Acid and Porphobilinogen in Urine. *J. Biol. Chem.* **1956**, *219*, 435–446.
30. Dailey HA, Dailey TA, Gerdes S, Jahn D, Jahn M, O'Brian MR, et al. Prokaryotic Heme Biosynthesis: Multiple Pathways to a Common Essential Product. *Microbiol. Mol. Biol. Rev.* **2017**, *81*, e00048-16.